Science Arts & Métiers (SAM)
is an open access repository that collects the work of Arts et Métiers Institute of Technology researchers and makes it freely available over the web where possible.

This is an author-deposited version published in: https://sam.ensam.eu
Handle ID: .http://hdl.handle.net/10985/10522

To cite this version :

Kerem EGE, Maxime GALLO, Jérôme ANTONI, Marc RÉBILLAT - Repeated exponential sine sweeps for the autonomous estimation of nonlinearities and bootstrap assessment of uncertainties - Journal of Manufacturing Science and Engineering - Vol. XX, n°XX, p.1-12 - 2015

Any correspondence concerning this service should be sent to the repository Administrator : scienceouverte@ensam.eu

Repeated exponential sine sweeps for the autonomous estimation of nonlinearities and bootstrap assessment of uncertainties

M. Rébillat [1], K. Ege[2], M. Gallo[2] and J. Antoni [2]

[1] PIMM, Arts et Métiers ParisTech / CNAM / CNRS, 151 Boulevard de l'Hôpital, 75013 Paris, FRANCE Email: marc.rebillat@ensam.eu
[2]Laboratoire Vibrations Acoustique, INSA-Lyon, 25 bis, avenue Jean Capelle, F-69621 Villeurbanne Cedex, France Email: kerem.ege@insa-lyon.fr

Abstract

Measurements on vibrating structures has been a topic of interest since decades. Vibrating structures are however generally assumed to behave linearly and in a noise-free environment, which is not the case in practice. This paper thus provides a methodology that allows for the autonomous estimation of nonlinearities and assessment of uncertainties by bootstrap on a given vibrating structure. Nonlinearities are estimated by means of a block-oriented nonlinear model approach based on parallel Hammerstein models and on exponential sine sweeps. Estimation uncertainties are simultaneously assessed using repetitions of the input signal (multi-sine sweeps) as the input of a bootstrap procedure. Mathematical foundations and practical implementation of the method are discussed on an experimental example. The experiment chosen here consists in exciting a steel plate under various boundary conditions with exponential sine sweeps and at different levels in order to assess the evolutions of nonlinearities and uncertainties over a wide range of frequencies and input amplitudes.

Keywords

Nonlinear vibrating structure, nonlinear system identification, parallel Hammerstein models, bootstrap procedure, uncertainty quantification.

1 Introduction

Vibrating structures are generally assumed to behave linearly and in a noise-free environment. This is in practice not perfectly the case. First, nonlinear phenomena such as jump phenomenon, hysteresis or internal resonance appear when the transverse vibration of a bi-dimensional structure exceeds amplitudes in the order of magnitude of its thickness [1]. Second, the presence of plant noise is a natural phenomenon that is unavoidable for all experimental measurements.

In order to perform reliable measurements of vibrating mechanical structures one should thus keep in mind these two issues and care about them. The first one, respectively *"nonlinearities"*, can be considered as a deterministic process in the sense that in the absence of noise the output signal depends only on the input signal. The second one, respectively *"noise"*, is purely stochastic: in the absence of an input signal, the output signal is not null and cannot be predicted at any arbitrary instant. At first, these two issues can be thought of as independent and solved by means of two distinct procedures. However, it turns out that they are actually coupled. Indeed, all the noise that is not correctly removed from the measurements could be misinterpreted as nonlinearities, thus polluting measurements. And if nonlinearities are not accurately estimated, they will end up within the noise signal and information about the structure under study will be lost. In this paper, we thus try to estimate nonlinearities while quantifying the uncertainties on these estimations that result from noise. The underlying idea consists in extracting the maximum of available linear and nonlinear deterministic information from measurements without misinterpreting noise.

The first problem addressed here is related to the estimation of nonlinear models of vibrating structures [2, 3]. Some approaches are based on a physical modeling of the structure whereas some perform without any physical assumption (black-box models). As nonlinear mechanisms in structures are complex and various and as we do not intend to build a model for each case, we choose to rely on black-box models. Among these black-box approaches, some assume a given form for the selected model (block-oriented models [4, 5, 6, 7]) whereas some do not put constraints on the model organization. Because block-oriented models can be interpreted easily, this class of models has been retained. A class of block-oriented models that is particularly interesting is the class of parallel Hammerstein models (see Fig. 1). It belongs to the class of *"Sandwich models"* [4] and is shown to possess a good degree of generality [2]. Moreover, thanks to exponential sine sweeps [8, 9, 10], nonparametric versions of such models can be very easily and rapidly estimated [11, 12]. The procedure developed recently for the nonparametric estimation of parallel Hammerstein models [11, 12] will thus be extended here in order to be able to take into account stochastic plant noise. This procedure has already proven to be very useful to study vibrating structures in various contexts [13, 14, 15].

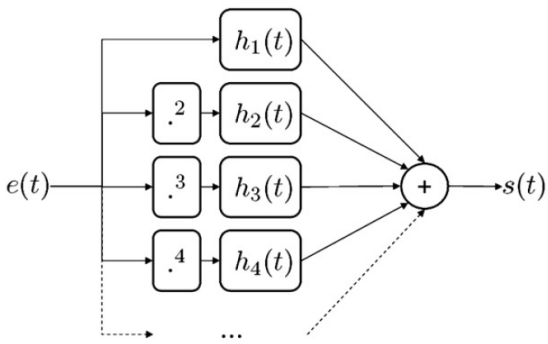

Figure 1: Representation of parallel Hammerstein models

The second problem addressed here is related to the estimation of uncertainties caused by the presence of noise in the context of nonlinear system estimation. Of prime importance for this issue is the design of the excitation signals. The use of special types of periodic excitations has been proved particularly advantageous in this respect [16]. A typical example is provided by multisines (i.e. a Fourier series with random phases) where some harmonics are voluntary removed. The detection of energy at the non-excited frequencies in the system response then provides a clear evidence of the presence of nonlinearites and also enables their quantification and, to some extent, their qualification (e.g. whether they correspond to odd or even orders). Another property of multisines is to allow the separation of nonlinearities from measurement noise. Several strategies towards this aim are described in reference [16]. They usually require the use of several multisine excitations with varying gains and/or randomly differing phases. In a recent work, a fast method was proposed to identify nonlinearities based on the use of a nonstationary excitation with an underlying periodic structure [17]. The idea was to progressively stear the system outside its linear range and at the same time to benefit from the properties of a multisine excitation to quantify the emergence of nonlinearities and separate out plant noise. The aim is here to demonstrate that the use of such a procedure based on multiple exponential sine sweeps will allow for a more robust and efficient estimation of nonlinear models of vibrating structures.

The aim of this paper is thus to provide a methodology that allows for the autonomous estimation of nonlinearities and uncertainties by bootstrap on a given vibrating structure. Nonlinearities are estimated by means of a block-oriented nonlinear model approach based on parallel Hammerstein models and on exponential sine sweeps [11, 12]. Estimation uncertainties are simultaneously assessed using repetitions of the input signal (multi exponential sine sweeps) as the input of a bootstrap procedure. Mathematical foundations and practical implementation of the method are discussed on an experimental example. The experiment chosen here consists in exciting a steel plate under various boundary conditions with exponential sine sweeps and at different levels in order to assess the evolutions of nonlinearities and to estimate uncertainties over a wide range of frequencies and input amplitudes. The paper is organized as follows. The original method developed for the nonparametric estimation of parallel Hammerstein models [11, 12] is first rapidly described in Sec. 2. Then, the benefits of the use of multiple exponential sine sweeps for the estimation of nonlinear models of vibrating structures is discussed in Sec. 3. Performances of the whole method are then illustrated experimentally on a vibrating plate in Sec. 4.

2 Identification of parallel Hammerstein models

This section aims at resuming the identification of parallel Hammerstein models by means of exponential sine sweeps, as initially proposed in Refs. [11, 12]. It introduces the quantities and notations that will be used later in the paper.

2.1 Parallel Hammerstein models

Volterra series are a convenient and general tool that provides an analytical expression of the relationship between the input $e(t)$ and the output $s(t)$ of a

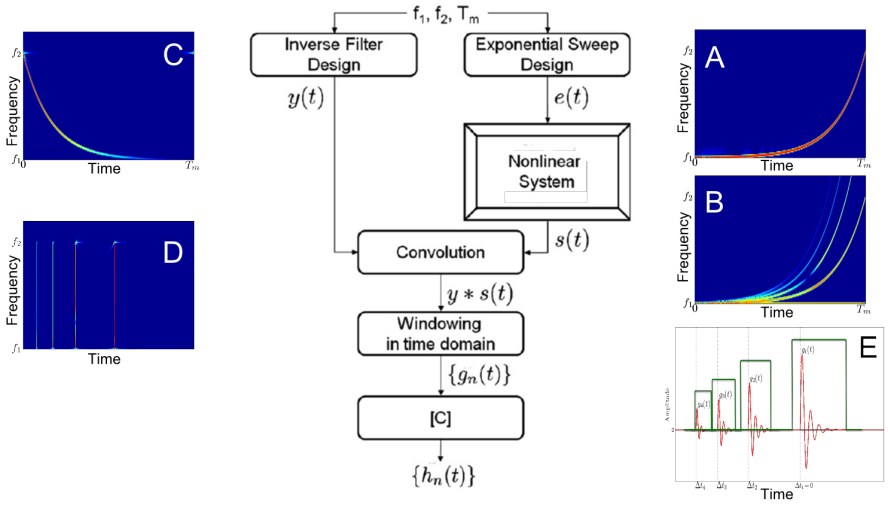

Figure 2: Schematic representation of the estimation procedure for parallel Hammerstein models based on exponential sine sweeps models [11, 12]. A: Generation of an exponential sine sweep $e(t)$ from parameters (f_1, f_2, T_m). B: Excitation of the nonlinear system and recording of the output signal $s(t)$. C: Generation of an inverse filter $y(t)$ from parameters (f_1, f_2, T_m). D: Convolution of the inverse filter $y(t)$ with the output signal $s(t)$. E: Extraction of intermediate values $\{g_n(t)\}$ by means of temporal windowing. Computation of $\{h_n(t)\}$ from $\{g_n(t)\}$ using the matrix $\boldsymbol{C}$.

weakly non-linear system [18]. A system is considered here as *"weakly"* nonlinear if it does not exhibit any discontinuous nonlinearity (such as a hard saturation for example). The class of weakly nonlinear systems is thus rather general and encompasses many real-life applications. Parallel Hammerstein models constitute an interesting subclass of Volterra systems [19, 2]. This class of model is very appealing as it is at the same time easy to estimate and to interpret as well as being mathematically still rather general.

In a parallel Hammerstein models [19, 2], each branch is composed of one nonlinear static polynomial element followed by a linear one, $h_n(t)$, as shown in Fig. 1. Mathematically, the relation between the input $e(t)$ and the output $s(t)$ of such a system is given by Eq. (1), where $*$ denotes the convolution product:

$$s(t) = \sum_{n=1}^{N} (h_n * e)^n(t). \tag{1}$$

In this model, each impulse response $h_n(t)$ is convolved with the input signal raised to its nth power and the output $s(t)$ is the sum of these convolutions. The first impulse response $h_1(t)$ represents the linear response of the system. The other impulse responses $\{h_n(t)\}_{n\in\{2\cdots N\}}$ model the nonlinearities. The family $\{h_n(t)\}_{n\in\{1\cdots N\}}$ will be referred to as the kernels of the model. Any parallel Hammerstein model is fully represented by its kernels.

2.2 Exponential sine sweeps

Estimating each kernel $h_n(t)$ of a parallel Hammerstein models is not a straightforward task. A simple estimation method that has been proposed previously [11, 12] for this purpose is briefly recalled here (see Fig. 2 for an overview of the method). To experimentally cover the frequency range over which the system under study has to be identified, cosines with time-varying frequencies are commonly used. When the instantaneous frequency of $e(t) = \cos[\phi(t)]$ is increasing exponentially from f_1 to f_2 in a time interval T, this signal is called an "Exponential Sine Sweep" (see Fig. 2.A). It can be shown [11, 12] that by choosing $T_m = (2m\pi - \pi/2)ln(\frac{f_2}{f_1})/2\pi f_1$ with $m \in \mathbb{N}^*$ one obtains the following property:

$$\forall n \in \mathbb{N}^*, \cos\left[n\phi(t)\right] = \cos\left[\phi(t + \Delta t_n)\right] \quad \text{with} \quad \Delta t_n = \frac{T_m \ln(n)}{\ln(\frac{f_2}{f_1})}. \tag{2}$$

Equation (2) states that for any exponential sine sweep of duration T_m, multiplying the phase by a factor n yields the same signal, advanced in time by Δt_n.

2.3 Kernel recovery in the time domain

If an exponential sine sweep is presented at the input of parallel Hammerstein models, by combining Eq. (1) and Eq. (2) and by using properties of Chebyshev polynomials (see Appendix), one obtains the following relation (see Fig. 2.B):

$$s(t) = \sum_{n=1}^{N} (g_n * e)^n (t + \Delta t_n) \quad \text{with} \quad g_n(t) = \sum_{n=1}^{N} \tilde{c}_{k,n} h_k(t) \tag{3}$$

where $g_n(t)$ can be interpreted as the contribution of the different kernels to the nth harmonic and $\tilde{c}_{k,n}$ is the coefficient (n, k) of the matrix $\tilde{\boldsymbol{C}}$. Details of the computation of the matrix $\tilde{\boldsymbol{C}}$ are provided in the Appendix.

In order to identify each kernel $h_n(t)$ separately, a signal $y(t)$ operating as the inverse of the input signal $e(t)$ in the convolution sense can be built as shown in [11, 12] (see Fig. 2.C). After convolving the output of Parallel Hammerstein models $s(t)$ given in Eq. (3) with $y(t)$, one obtains Eq. (4) (see Fig. 2.D) :

$$(y * s)(t) = \sum_{n=1}^{N} g_n(t + \Delta t_n). \tag{4}$$

Because $\Delta t_n \propto \ln(n)$ and $f_2 > f_1$, the higher the order of nonlinearity n, the more advanced is the corresponding $g_n(t)$. Thus, if T_m is chosen long enough, the different $g_n(t)$ do not overlap in time and can be separated by simply windowing them in the time domain (see Fig. 2.E). Using Eq. (3), the family $\{h_n(t)\}_{n \in \{1 \cdots N\}}$ of the kernels of the parallel Hammerstein models under study can then be fully extracted as

$$[h_1(t) \cdots h_N(t)]^T = \tilde{\boldsymbol{C}}[g_1(t) \cdots g_N(t)]^T. \tag{5}$$

2.4 Advantages and limitations of the method

The method described here [11, 12] thus easily provides a direct mathematical access to all the kernels of a parallel Hammerstein model. The main advantage of this exponential sine sweep based method is to be fast and simple: using only one exponential sine sweep one can have direct access to the kernels of an arbitrary vibrating device without the need of any complicated signal processing procedure (see Fig. 2).

The method presented here is not exactly the same as the standard sine sweep method [8, 9]. It can be thought as similar as the input signal being used is still a sine sweep. However, the sine sweep used here has to satisfy some specific additional requirements. First of all, the input sine sweep must have its frequency varying exponentially with time. Secondly, the length of the exponential sine sweep cannot be set arbitrarily and must be chosen among a given set of admissible values. Finally, the two methods do not have the same purpose. With the standard sine sweep method, the aim is to estimate the linear impulse response of a given system while being robust to nonlinearities. With the proposed method, the aim is to estimate a whole nonlinear model of the system under study. The method presented here can thus be thought as an extension of the standard sine sweep method.

However, this method still needs to be improved to some extent. The main limitation lies in its unability to distinguish between nonlinearities and experimental noise. This results in an overestimation of the nonlinear behavior as estimated kernels also include some plant noise. Another limitation of this method is related to the parameter N that denotes the number of kernels (or equivalently the number of branches) to be estimated in the parallel Hammerstein models. For the moment this parameter is chosen arbitrarily or by using some empirical rules and efforts have to be done to estimate it automatically. These questions constitute the main topics of this paper and will be addressed in the following section.

Finally, recent studies [20, 21] have shown that distortion artifacts can appear in the causal part of the impulse responses estimated by means of exponential sine sweep when the system under study is not perfectly modeled by parallel Hammerstein blocks. Indeed, in practical applications one will never face a system that is exactly a parallel Hammerstein model as this kind of system corresponds to a mathematical idealization. In this situation the method proposed here will thus unavoidably return some sort of artefact present in the causal part of the estimated impulse responses. However, as mentioned by references [20, 21] those artifacts remain of very small amplitude.

3 Estimation uncertainties

The identification method described in the previous section originally used a single sweep for the excitation signal, as described by Eq. (2). Although this is enough to decompose the system output into nonlinear contributions of different orders, it does not allow for the estimation of uncertainties. This may be troublesome when weak nonlinearities – typically related to higher-order kernels – are highly contaminated by plant noise. Inspired from Refs. [16, 17], a simple solution to alleviate this situation is to repeat the same exponential sine sweep

several times so as to excite the system with a periodic signal. By taking advantage of repeated experiments, it is then possible to estimate the contribution of plant noise by synchronous averaging. The use of the synchronous average on repeated experiments is not a novel contribution as such; yet, when combined in a certain manner with the exponential sine sweep method, it provides rather unique and simple ways 1) to automatically test for the determination of the effective number of kernels to estimate and 2) to assess estimation uncertainties on the nonlinear kernels by use of the bootstrap. These issues are discussed in the following subsections.

3.1 Noise estimation by synchronous averaging

The principle is to repeatedly excite the system with the same sine sweep $e_0(t)$. The input signal then reads $e(t) = \sum_{k=0}^{K-1} e_0(t - kT_m)$, with K periods of duration T_m indexed by k (see Sec. 2.2 for the definition of T_m). A property of non-linear systems described by parallel Hammerstein branches is to respond with a periodic output sharing the same period T as the input (PISPO system: Period In Same Period Out). The same property obviously holds for the deconvolved signal. Specifically, let

$$x(t) = g(t) + n(t) \tag{6}$$

denote the noisy counterpart of Eq. (4) where $g(t) = (y * s)(t) = \sum_{n=1}^{N} g_n(t + \Delta t_n)$ has now been periodized such that $g(t) = g(t - T_m)$ and $n(t)$ stands for plant noise.

The aim is now to separate $g(t)$ from $n(t)$. Since the system output is theoretically periodic in the absence of noise, a natural estimate of it is provided by the synchronous average

$$\hat{g}(t) = \frac{1}{K} \sum_{k=0}^{K-1} x(t - kT_m) \tag{7}$$

and, by subtraction, an estimate for plant noise is

$$\hat{n}(t) = x(t) - \hat{g}(t). \tag{8}$$

Note that these estimates hold whatever the probability and power spectral distributions of the noise provided that it is uncorrelated from one period to another. In addition, it is readily checked that they are unbiased. Given a number K of periods of the same sweep, the variance of $\hat{g}(t)$ can be shown to be equal to σ_n^2/K with σ_n^2 the variance of plant noise of which an estimate at time t is returned by

$$\hat{\sigma}_n^2(t) = \frac{1}{K} \sum_{k=0}^{K-1} \hat{n}(t - kT_m)^2. \tag{9}$$

Therefore, the noise-to-signal ratio (NSR) of the synchronous average decreases proportionally with K. Specifically, by defining

$$\mathrm{NSR}(K) = 20 \log_{10} \left(\frac{\mathrm{RMS}(\hat{g} - g)}{\mathrm{RMS}(\hat{g})} \right), \tag{10}$$

the NSR based on K averages (wherein RMS(z) stands for the Root-Mean-Square value of signal $z(t)$), one has the simple relationship

$$\mathrm{NSR}(K) = \mathrm{NSR}(1) - 3 \cdot \log_2(K) \tag{11}$$

where $\mathrm{NSR}(1) = \mathrm{RMS}(n)/\mathrm{RMS}(x)$ is the initial NSR. Therefore, the NSR decreases by 3 dB when doubling the number of averages. However, even if this formula may suggest that noise disappears when increasing the number of averages, one should keep in mind that noise will never be completely eliminated from finite-length measurements.

Using the synchronous average $\hat{g}(t)$ in place of $g(t)$ in the identification method of section 2 will obviously decrease the uncertainties on the estimation of the non-linear kernels $h_n(t)$. However, despite the NSR being decreased, the complete removal of noise is not possible (as long as $K < \infty$) and it still remains to assess the limit where weak nonlinearities can be statistically distinguished from noise and the corresponding uncertainties estimated. These two issues are addressed in the following two subsections.

3.2 Autonomous determination of the number of kernels

The principle of the exponential sine sweep based method is rooted on the detection of the nth order harmonic contributions $g_n(t)$, $n = 1, ..., N$ in the time-domain. As illustrated in Fig. 2.E, it might not be obvious at first to determine how many $g_n(t)$'s have been excited when higher-order ones are likely to be masked by noise.

However, the determination of the correct number N of harmonic contributions is crucial to return unbiased estimates [11]. This is due to the fact that the kernels $h_n(t)$ to be estimated are depending on all identified harmonic contributions $g_k(t)$, $k = 1, ..., N$, as seen by inverting the second formula in Eq. (3). Too small a number would result in underestimating the nonlinearities in the system. On the contrary, too large a number would considerably increase estimation noise.

An autonomous procedure is proposed that determines the effective number of kernels which can be distinguished from plant noise. It is based on the following statistical F-test. Let's consider the synchronous average $\hat{g}(t)$ in a short time interval $\mathcal{I}_n$ centered around the expected occurrence of the n-th kernel, i.e. $t \in \mathcal{I}_n = [t_{n,1}, ..., t_{n,2}]$ with $\Delta t_n \leq t_{n,1}$ and $t_{n,2} < \Delta t_{n-1}$. The question is whether $\hat{g}(t)$ significantly protrudes from background noise in that interval – and therefore originates from a n-th nonlinearity – or whether it is mainly noise (see Fig. 6). This corresponds to two alternative hypotheses:

- H0: $\hat{g}(t), t \in \mathcal{I}_n$ is plant noise only
- H1: $\hat{g}(t), t \in \mathcal{I}_n$ contains an nth order harmonic contribution $g_n(t)$.

Following the analysis of section 3.1 and making use of Eq. (9), an estimate of the variance in interval $\mathcal{I}_n$ under H0 is returned by

$$\hat{\sigma}^2_{\mathcal{I}_n|H0} = \frac{1}{t_{n,2} - t_{n,1} + 1} \sum_{t=t_{n,1}}^{t_{n,2}} \frac{1}{K} \hat{\sigma}^2_n(t) \tag{12}$$

(note the division by K since the level of noise on the synchronous average is K times as small as on the initial signal according to formula (11)). Therefore, assumption H0 is to be rejected if the current "variance"

$$\hat{\sigma}^2_{\mathcal{I}_n} = \frac{1}{t_{n,2} - t_{n,1} + 1} \sum_{t=t_{n,1}}^{t_{n,2}} \hat{g}(t)^2 \tag{13}$$

is found statistically greater than $\hat{\sigma}^2_{\mathcal{I}_n|H0}$. This can be easily formalized with a F-test for the equality of two variances: H0 is rejected if the ratio $\hat{\sigma}^2_{\mathcal{I}_n}/\hat{\sigma}^2_{\mathcal{I}_n|H0}$ is greater than $F(\alpha)_{K-1,K-1}$, the critical value of the F distribution with $K-1$ and $K-1$ degrees of freedom and a significance level of α.

The highest-order harmonic contribution $g_N(t)$ that is found significant through this procedure then determines the model order N.

3.3 Bootstrap assessment of uncertainties

Eventually, the use of repeated exponential sine sweeps also gives access to the uncertainties on the non-linear kernels $h_n(t)$. Even if a full analytic treatment of the question is possible in the case of Gaussian noise, a resampling strategy based on the bootstrap is preferred due to its simplicity and versatility with respect to unknown noise properties [22].

The bootstrap is a technique to artificially produce random repetitions of the experiment from the available data. The aim is to obtain an histogram for the estimated kernels $h_n(t)$ from which confidence intervals (or any other measure of statistical dispersion related to uncertainties) can easily be constructed. This is achieved by producing a series of virtual repetitions of the same experiment. Let $x_k(t) = x(t - kT_m)$, $0 \leq t < T_m$, denote the k-th cycle of signal $x(t)$ (as defined in Eq. (6)) and π a random draw of the integers $0, ..., K-1$ (i.e. each element $\pi(i)$, $i = 0, ..., K-1$, is randomly assigned a value of set $0, ..., K-1$ with uniform probability $1/K$). A new virtual measurement $x^{(b)}(t)$ (where $^{(b)}$ denotes the bootstrap index and is not to be confused with an exponentiation) is then produced by concatenating K random draws with replacement,

$$\left\{x_{\pi(0)}(t); ...; x_{\pi(K-1)}(t)\right\}. \tag{14}$$

from which the synchronous average

$$\hat{g}^{(b)}(t) = \frac{1}{K} \sum_{k=0}^{K-1} x_{\pi(k)}(t) \tag{15}$$

is computed. By means of an example with $K = 3$, one possible bootstrap draw, say $b = 1$, would return $\{\pi(0); \pi(1); \pi(2)\} = \{2, 1, 1\}$ and therefore $\hat{g}^{(1)}(t) = \frac{1}{3}(x_2(t) + x_1(t) + x_1(t))$; another draw would return $\{\pi(0); \pi(1); \pi(2)\} = \{0, 2, 0\}$ and therefore $\hat{g}^{(2)}(t) = \frac{1}{3}(x_0(t) + x_2(t) + x_0(t))$, etc ...

Next, for each bootstrapped synchronous average $\hat{g}^{(b)}(t)$ a new estimate $h_n^{(b)}(t)$ is obtained by following the procedure of Sec. 2. This is repeated B times such as to collect B estimates $h_n^{(b)}(t)$, $b = 1, ..., B$, from which a histogram can finally be calculated. Similarly, histograms are available on any transform of the estimated kernels, in particular on their Fourier transforms as displayed in

Sec. 4. Specifically, by denoting $H_n^{(b)}(f)$ the Fourier transform of the bootstrap estimate of the n-th kernel $h_n^{(b)}(t)$ from a random draw b, the uncertainties in the frequency domain are evaluated by the difference

$$U_n^{(b)}(f) = H_n^{(b)}(f) - \frac{1}{B}\sum_{b=0}^{B-1} H_n^{(b)}(f). \tag{16}$$

The mean square uncertainty on the n-th kernel based on K averages may then be defined as

$$\mathrm{MSU}_n(f,K) = \frac{1}{B}\sum_{b=0}^{B-1} |U_n^{(b)}(f)|^2. \tag{17}$$

Finally, the uncertainty-to-signal ratio (USR) can be defined as:

$$\mathrm{USR}_n(K) = \frac{\int \mathrm{MSU}_n(f,K)df}{\int \frac{1}{B}\sum_{b=0}^{B-1} |H_n^{(b)}(f)|^2 df} \tag{18}$$

where the integrals are taken over the full frequency band of interest.

This index can be interpreted as a compact way to assess the quality of the estimated kernels and can be compared to NSR(K) as defined in Eq. (11). NSR(K) stands for the ratio of the energy of the noise versus the energy of the estimated signal for K repetitions of the exponential sine sweep. $\mathrm{USR}_n(K)$ denotes the ratio of the energy of the uncertainty on the nth kernel versus the energy of the estimated n^{th} kernel for K repetitions of the exponential sine sweep. As the uncertainty on the nth kernel may be linked with the variance of noise, a correlation between both indexes is to be expected.

Note that the bootstrap is a computer intensive method. Yet it was found reasonably fast to run for values of B up to the order of a few hundreds.

4 Application to a vibrating plate

4.1 Experimental setup

In order to illustrate the performance of the proposed extended exponential sine sweep method, vibratory measurements have been done on a simple mechanical system. The chosen structure is a thin rectangular steel plate of $540 \times 640 \times 1$ mm^3 dimensions. An electrodynamic mini-shaker (B&K Type 4810) is used to excite the plate at a point chosen arbitrarily (see Fig. 3). Acceleration of the plate is measured at two positions: at the driving point through an impedance head (PCB Type 288D01) and at several centimeters from it using a second accelerometer (B&K Type 4508). Two configurations have been tested:

- in the first one (see Fig. 3(a)) the plate is clamped at edges with four metal bars (of 2 cm width) screwed to the top ledges of a cavity of $500 \times 600 \times 700$ mm^3 dimensions.
- in the second configuration (see Fig. 3(b)) the plate is suspended (boundary conditions can be supposed as free) and highly damped by adding a porous material glued on one face of the plate.

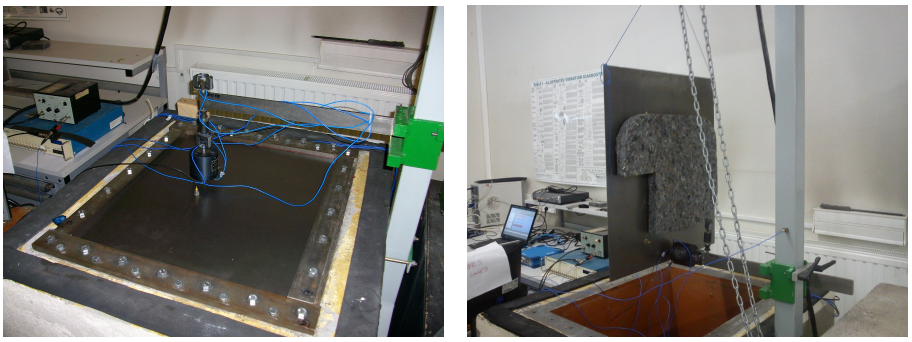

(a) (b)

Figure 3: Overview of the experimental setup. (a) First configuration: steel plate coupled to a cavity (*clamped* boundary conditions). (b) Second configuration: suspended damped plate (*free* boundary conditions).

The extended exponential sine sweep method presented here has been applied to these two different configurations. The aim is not to compare the amount of nonlinearities for different test cases or to discuss the relative results of different experimental configurations, but simply to show how the methodology can be easily applied to examples of common engineering problems which may arise in the vibroacoustic community: a typical lightly damped clamped structure and a highly damped "free-free" one. These two systems with different boundary conditions and different amounts of damping exhibit different levels of nonlinearities from different origins (geometrical nonlinearities, contacts, ...).

For each configuration the plate is excited with 20 exponential sine sweeps of 30 sec each, repeated periodically. The instantaneous frequency of the sweep increases from 20 Hz to 1 kHz. The sampling frequency is fixed at 25.6 kHz in order to allow for the estimation of high order kernels. Several measurements at different gains have been performed in order to assess the evolutions of nonlinearities and of the signal to noise ratio over a wide range of frequencies and input amplitudes.

4.2 Assessment of estimation uncertainties

This subsection illustrates the assessment of estimation uncertainties by means of the bootstrap technique described in Sec. 3.3. The signal under study corresponds to the second accelerometer (glued on the plate several centimeters away from the impedance head) for the first configuration where the plate is clamped (see Fig. 3(a)). It contains a maximum of $K_{max} = 20$ repetitions of the response of the system to exponential sine sweeps. During the first repetition the system is considered to exhibit a transient response while it reaches its stationary regime when the second repetition of the sweep is starting up. For that reason, the first repetition has been removed from the analysis. The objective is here to demonstrate the USR (see Eq. (18)) improvement caused by the synchronous averaging process.

Figures 4(a) and 4(b) display the effect of the synchronous average over $K = 19$ repetitions of the exponential sine sweep – as compared to $K = 1$

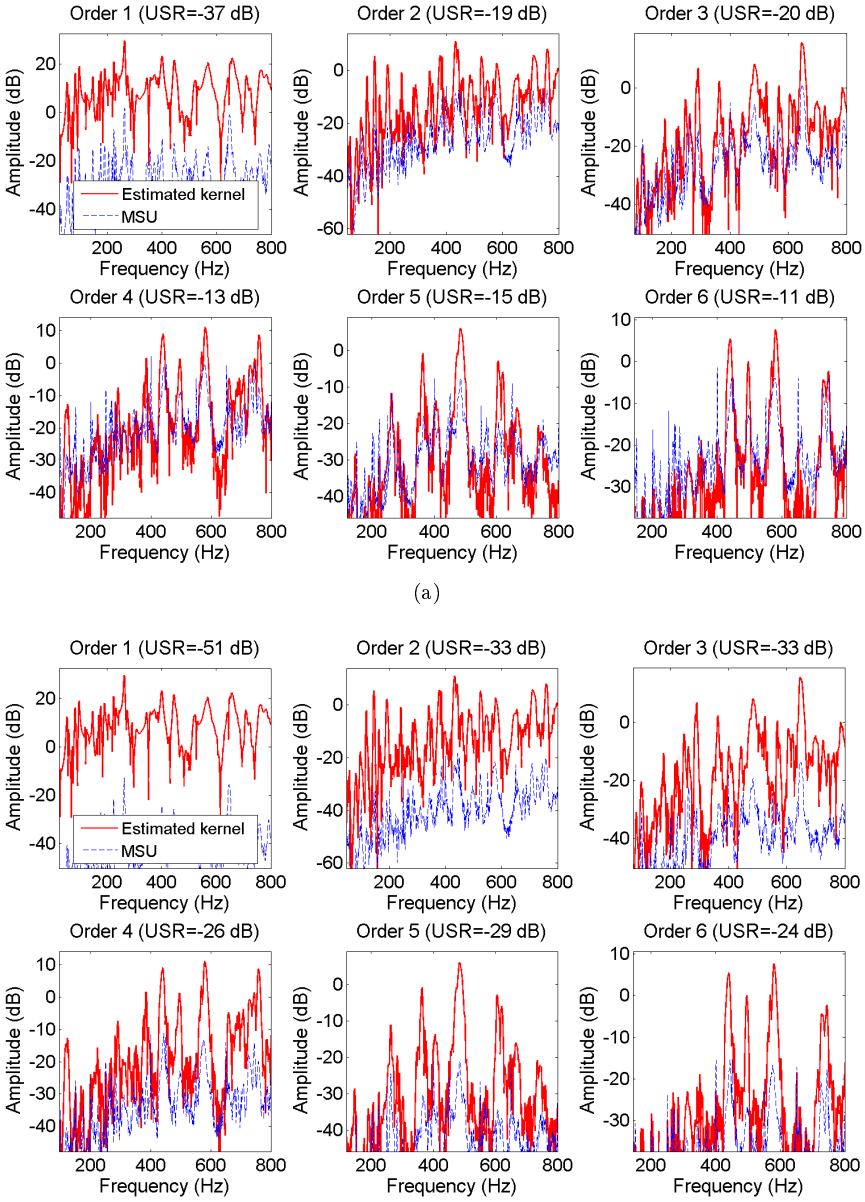

Figure 4: Illustration of the USR improvement implied by synchronous averaging. a) Frequency gains of kernels estimated on one period of the excitation signal together with the mean square uncertainty obtained classically. b) Frequency gains of kernels estimated by synchronously averaging $K = 19$ periods of the excitation signal together with the mean square uncertainty $\mathrm{MSU}_n(f, 19)$ obtained by bootstrap ($B = 150$ random draws with replacement).

– for the estimation of non-linear kernels up to order $N = 6$. The estimated kernels are displayed in each figure together with the corresponding mean square uncertainty MSU(f, K) of Eq. (17) as obtained from bootstrap. One can clearly see the benefit of reducing the noise by synchronous averaging, especially for the high-orders kernels for which the initial USR without averaging is very low (-11 dB for the 6th order kernel for example) and becomes acceptable after averaging (-23 dB for the 6th order kernel). Moreover, comparison of Figs. 4(a) and 4(b) displays a reduction of $\simeq 13$ dB of the estimation uncertainties for each kernel order, which is very close to the value predicted by Eq. (11). Figure 5 then illustrates the improvement with respect to K of both the NSR as given by Eq. (11) and the USR as given by Eq. (18). As expected, the curves evidence an excellent correlation between both indexes.

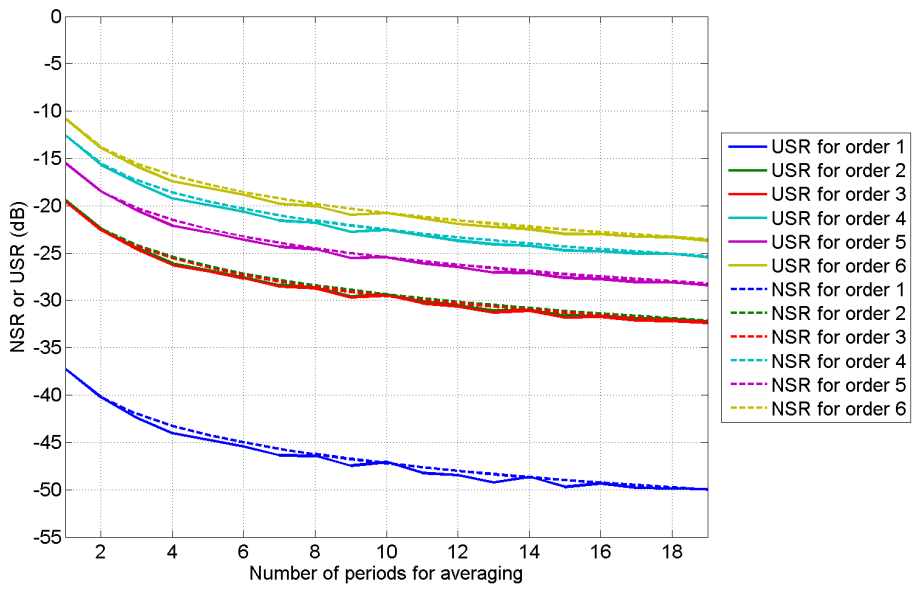

Figure 5: Improvement with respect to K of both the NSR as given by Eq. (11) and the USR as given by Eq. (18).

4.3 Determination of the effective number of kernels

This section illustrates the automatic determination of the effective number of kernels N_{opt} as explained in Sec. 3.2. Measurements are now performed on the second configuration (suspended damped plate, see Fig. 3(b)). The signal studied here corresponds to the second accelerometer, after synchronous averaging on all periods except the first one (transient regime). Four gains for the excitation signal are successively tested $G = 0.1 - 1 - 5$ and 10 in order to study the robustness of the determination method to predict the proper number of kernels to estimate. For the fourth gain ($G = 10$), the excitation force delivered from the shaker is one hundred times higher than for the first gain ($G = 0.1$). For example, in terms of displacement, at a resonance frequency around 130 Hz and at the point of measurement of the second accelerometer (several

centimeters away from the shaker), the gain $G = 0.1$ creates a displacement of about 5 μm whereas the gain $G = 10$ generates a displacement of about 0.5 mm, that is half the plate thickness (1 mm). It is obvious that with such large-amplitude vibration motions, geometrical nonlinearities appear strongly with high order kernels being excited.

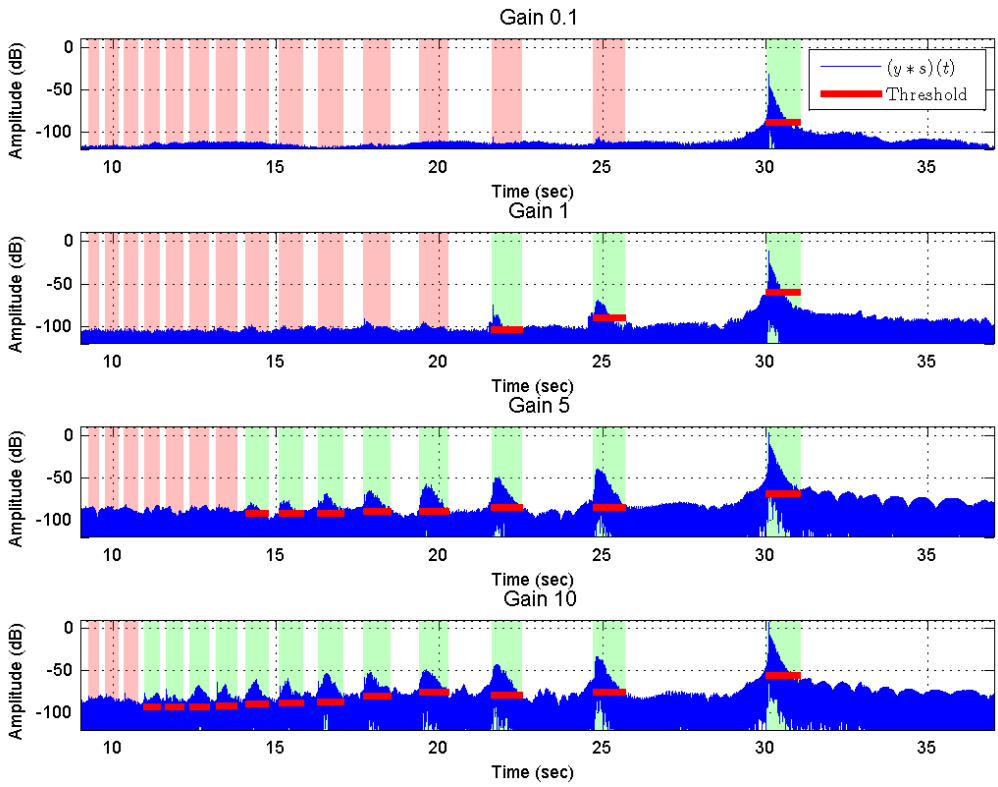

Figure 6: Illustration of the determination of the effective number of kernels for the second configuration (suspended damped plate, see Fig.3(b)) for four different excitation gains ($G = 0.1 - 1 - 5 - 10$). The signal $|g(t)| = |(y * s)(t)|$ (output signal after deconvolution, see Eq. (4)) in the time domain is displayed in dB in blue and the selection thresholds in red. Retained kernels are displayed with green windows, and rejected ones with red windows.

In Fig. 6, the determination of the effective number of kernels (using the methodology presented in Sec. 3.2) is illustrated in the time-domain on the signal $g(t) = (y * s)(t)$ (output signal after deconvolution, see Eq. (4)). The thresholds defined in Sec. 3.2 (through F-test at 0.995 and with a security parameter chosen equal to 6) is displayed in red lines in Fig. 6 together with the intervals $\mathcal{I}_n$ which are materialized by the vertical shaded areas. These thresholds allow estimation of the effective number of kernels to retain for each excitation level. Green windows are displayed for retained kernels and red windows for rejected ones. As expected, the optimal model order N_{opt} of retained kernel increases with the level of excitation: $N_{\text{opt}} = 1 - 3 - 8$ and 12 respectively. These estimated kernels are presented in Fig. 7 for each gain. One can note that the level of the kernels

increases with the excitation gain. Moreover, the frequency content of the first kernel (corresponding to the linear part) is very similar for each measurement, thus assessing the reproducibility and precision of the measurements. To sum it up, the methodology presented here is a useful tool to select the proper model order N_{opt} and a major improvement of such nonlinearity estimation methodologies.

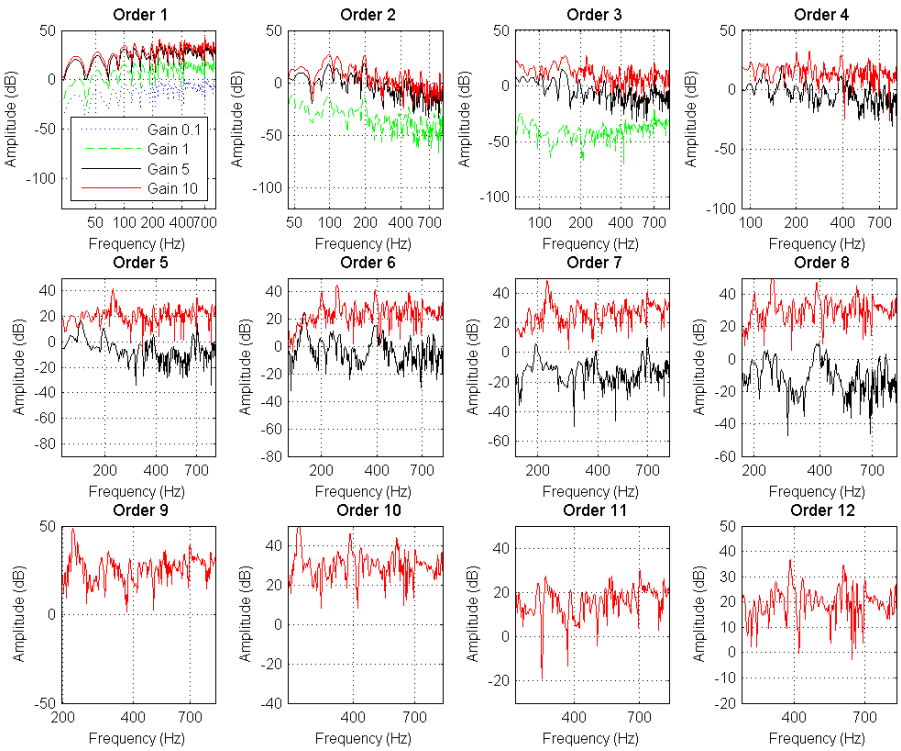

Figure 7: Estimated kernels for the second configuration (suspended damped plate, see Fig.3(b)) after determination of the effective number of kernels for each of the four excitation levels.

5 Conclusion

The aim of this paper is to provide a methodology that allows for the autonomous estimation of nonlinearities and of uncertainties by bootstrap on a given vibrating structure. Nonlinearities are estimated by means of a block-oriented nonlinear model approach based on parallel Hammerstein models and on exponential sine sweeps. Estimation uncertainties are simultaneously assessed using repetitions of the input signal (multi-sine sweeps) as the input of a bootstrap procedure. Mathematical foundations and practical implementation of the method are discussed on an experimental example. The experiment chosen here consists in exciting a steel plate under various boundary conditions

with exponential sine sweeps and at different levels, in order to assess the evolutions of nonlinearities and of the signal-to-noise ratios over a wide range of frequencies and input amplitudes.

The major improvements provided in this article are:

- the fact that the synchronous average allows the design of a simple statistical test to automatically determine the effective number of non-linear kernels in the exponential sine sweep method (in a manner that is actually quite unique to this method),
- the fact that the synchronous average is combined with the bootstrap to propose a versatile technique for assessing the uncertainties on any quantity of interest by taking advantage of repeated measurements.

6 Acknowledgments

Since 2011, the Laboratoire Vibrations Acoustique is part of the LabEx CeLyA of Université de Lyon, operated by the French National Research Agency (ANR-10-LABX-0060/ ANR-11-IDEX-0007). Part of this work was presented at the NOVEM 2015 conference (NOise and Vibration: EMerging technologies) [23].

Appendix: Computation of the matrix $\tilde{C}$

Chebyshev polynomials $\{T_k[\cos(\phi)]\}_{k\in\mathbb{N}}$ are defined by Eq. (19).

$$\forall k \in \mathbb{N}, \cos(k\phi) = \quad T_k[\cos(\phi)] \tag{19}$$

Subsequently, it can easily be shown that they satisfy the recurrence relation given in Eq. (20).

$$k = 0 \qquad T_0(x) = 1 \tag{20a}$$
$$k = 1 \qquad T_1(x) = x \tag{20b}$$
$$k > 1 \qquad T_{k+1}(x) = 2xT_k(x) - T_{k-1}(x) \tag{20c}$$

Then, by writing the polynomials as in Eq. (21) , one can obtain Eq. (22), using Eq. (20), and find the coefficients of the matrix $\boldsymbol{A}$.

$$T_k(x) = \sum_{i=0}^{k} A(i,k)x^i \tag{21}$$

$$i = 0 \qquad A(0,k+1) = -A(0,k-1) \tag{22a}$$
$$0 < i < k \qquad A(i,k+1) = 2A(i-1,k) - A(i,k-1) \tag{22b}$$
$$i \geqslant k \qquad A(i,k+1) = 2A(i-1,k) \tag{22c}$$

The linearisation of the polynomials can now be rewritten in a matrix form, as in Eq. (23).

$$\begin{bmatrix} 1 \\ \cos(x) \\ \dots \\ \cos(Nx) \end{bmatrix} = \boldsymbol{A} \begin{bmatrix} 1 \\ \cos(x) \\ \dots \\ \cos^N(x) \end{bmatrix} \tag{23}$$

Inverting Eq. (23) results in Eq. (24) which gives explicitly the $\boldsymbol{C}$ matrix.

$$\boldsymbol{C} = \boldsymbol{A}^{-1} \tag{24}$$

The matrix $\tilde{\boldsymbol{C}}$, necessary to access to $\{h_n(t)\}_{n\in[1,N]}$, is the matrix $\boldsymbol{A}$ without the first column and the first row, as seen in Eq. (5). To avoid the implementation of the recurrence, the $\tilde{\boldsymbol{C}}$ matrix of order 8, which is sufficient for practical use, is given in Eq. (25).

$$\tilde{\boldsymbol{C}} = \begin{bmatrix} 1 & 0 & -3 & 0 & 5 & 0 & -7 & 0 \\ 0 & 2 & 0 & -8 & 0 & 18 & 0 & -32 \\ 0 & 0 & 4 & 0 & -20 & 0 & 56 & 0 \\ 0 & 0 & 0 & 8 & 0 & -48 & 0 & 160 \\ 0 & 0 & 0 & 0 & 16 & 0 & -112 & 0 \\ 0 & 0 & 0 & 0 & 0 & 32 & 0 & -256 \\ 0 & 0 & 0 & 0 & 0 & 0 & 64 & 0 \\ 0 & 0 & 0 & 0 & 0 & 0 & 0 & 128 \end{bmatrix} \tag{25}$$

References

[1] C. Touzé, O. Thomas, and A. Chaigne. Asymmetric non-linear forced vibrations of free-edge circular plates. part 1: Theory. *Journal of Sound and Vibration*, 258(4):649–676, 2002.

[2] R. K. Pearson. *Discrete-Time Dynamic Models*. Oxford University Press, 1999.

[3] G. Kerschen, K. Worden, A. F. Vakakis, and J. C. Golinval. Past, present and future of nonlinear system identification in structural dynamics. *Mechanical Systems and Signal Processing*, 20(3):505–592, April 2006.

[4] H. W. Chen. Modeling and identification of parallel nonlinear systems: Structural classification and parameter estimation methods. *Proceedings of the IEEE*, 83(1):39–66, 1995.

[5] A. Janczak. *Identification of Nonlinear Systems using Neural Networks and Polynomial Models: A Block-Oriented Approach*. Springer, 2005.

[6] F. Giri and Er-Wei Bai. *Block-Oriented Nonlinear System Identification*. Springer, 2010.

[7] J. Schoukens, R. Pintelon, Y. Rolain, M. Schoukens, K. Tiels, L. Vanbeylen, A. Van Mulders, and G. Vandersteen. Structure discrimination in block-oriented models using linear approximations: A theoretic framework. *Automatica*, 53:225–234, March 2015.

[8] S. Muller and P. Massarani. Transfer-function measurement with sweeps. *Journal of the Audio Engineering Society*, 49(6):443–471, 2001.

[9] G. B. Stan, J. J. Embrechts, and D. Archambeau. Comparison of different impulse response measurement techniques. *Journal of the Audio Engineering Society*, 50(4):249–262, 2002.

[10] P. Majdak, P. Balazs, and B. Laback. Multiple exponential sweep method for fast measurement of head-related transfer functions. *Journal of the Audio Engineering Society*, 55(7-8):623–637, 2007.

[11] M. Rébillat, R. Hennequin, E. Corteel, and B. F.G. Katz. Identification of cascade of hammerstein models for the description of nonlinearities in vibrating devices. *Journal of sound and vibration*, 330:1018–1038, 2011.

[12] A. Novak, L. Simon, F. Kadlec, and P. Lotton. Nonlinear system identification using exponential swept-sine signal. *IEEE Transactions On Instrumentation and Measurement*, 59(8):2220–2229, August 2010.

[13] K. Ege, X. Boutillon, and M. Rébillat. Vibroacoustics of the piano soundboard: (non)linearity and modal properties in the low- and mid-frequency ranges. *Journal of Sound and Vibration*, 332(5):1288–1305, 2013.

[14] A. Novak, M. Bentahar, V. Tournat, R. El Guerjouma, and L. Simon. Nonlinear acoustic characterization of micro-damaged materials through higher harmonic resonance analysis. *NDT & E International*, 45(1):1–8, January 2012.

[15] M. Rébillat, R. Hajrya, and N. Mechbal. Nonlinear structural damage detection based on cascade of hammerstein models. *Mechanical Systems and Signal Processing*, (in press), 2014.

[16] R. Pintelon and J. Schoukens. *System Identification: A Frequency Domain Approach*. IEEE-press, Piscataway, 2001.

[17] E. Zhang, J. Antoni, R. Pintelon, and J. Schoukens. Fast detection of system nonlinearity using nonstationary signals. *Mechanical Systems and Signal Processing*, 24:2065–2075, 2010.

[18] S. Boyd and L. O. Chua. Fading memory and the problem of approximating nonlinear operators with volterra series. *IEEE Transactions on Circuits and Systems*, 32(11):1150–1161, 1985.

[19] P. G. Gallman. Iterative method for identification of nonlinear-systems using a Uryson model. *IEEE Transactions on Automatic Control*, 20(6):771–775, 1975.

[20] A. Torras-Rosell and F. Jacobsen. A new interpretation of distortion artifacts in sweep measurements. *Journal of the Audio Engineering Society*, 59(5):283–289, 2011.

[21] D. G. Ciric, M. Markovic, M. Mijic, and D. Sumarac-Pavlovic. On the effects of nonlinearities in room impulse response measurements with exponential sweeps. *Applied Acoustics*, 74(3):375–382, March 2013.

[22] A. M. Zoubir and D. R. Iskander. *Bootstrap Techniques for Signal Processing*. Cambridge University Press, 2007.

[23] M. Gallo, K. Ege, M. Rébillat, and J. Antoni. A multi-sine sweep method for the characterization of weak non-linearities; plant noise and variability estimation. In *NOVEM, 2015 Dubrovnik, Croatia.*